Semiconductor Physics, Quantum Electronics & Optoelectronics, 2025. V. 28, No 1. P. 109-120.

Sensors

Enhancement of sensory properties of chemoresistive conductive nanocomposites of carbon nanotubes and polypyrrole by functionalized calixarenes

A.A. Pud[1,*], Yu.V. Noskov[1], N.A. Ogurtsov[1], O.L. Kukla[2], O.S. Kruglyak[1], A.V. Mamykin[2], S.O. Cherenok[3], S.G. Vyshnevskyy[3], V.I. Kalchenko[3]

[1]*V. Kukhar Institute of Bioorganic Chemistry and Petrochemistry, NAS of Ukraine*
50 Kharkivske Highway, 02160 Kyiv, Ukraine
[2]*V. Lashkaryov Institute of Semiconductor Physics, NAS of Ukraine*
41 Nauky Avenue, 03028 Kyiv, Ukraine
[3]*Institute of Organic Chemistry, NAS of Ukraine*
1 Academician Kukhar Street, 02660 Kyiv, Ukraine
[*]*Corresponding author e-mail: alexander.pud@gmail.com*

Abstract. This work presents for the first time the modification and enhancement of sensory properties of a chemoresistive conductive core-shell nanocomposite of multi-walled carbon nanotubes (MWCNTs) and polypyrrole (PPy) doped by *p*-toluenesulfonate anions (TS) (MWCNT/PPy-TS) under long ultrasonic treatment in joint dispersions and, hence, under physico-chemical interactions with functionalized calixarenes (CA), namely calix[4]arene methylene-bis-phosphonic acid octasodium salt (CPA) and calix[4]arene sulfonic acid (CSA). The interactions are confirmed by a detailed analysis of FTIR spectra of a parent binary MWCNT/PPy-TS nanocomposite and its counterpart ternary MWCNT/PPy-TS/CA nanocomposites as well as by sensor measurements. The results of the latter show a strong enhancement of the sensitivity of the MWCNT/PPy-TS to isopropanol, acetone and ammonia vapors due to CSA and CPA additives, which, however, depends on the nature of functional groups of these CA.

Keywords: sensor nanocomposites, carbon nanotubes, polypyrrole, calix[4]arenes, interactions, sensitivity enhancement.

https://doi.org/10.15407/spqeo28.01.109
PACS 07.07.Df, 61.48.De

Manuscript received 14.01.25; revised version received 24.02.25; accepted for publication 12.03.25; published online 26.03.25.

1. Introduction

Identification (sensing) of volatile organic and inorganic compounds (VOC and VIC) by chemoresistive gas sensors is realized, in fact, through adsorption of these compounds at the surface of a sensing material. Such adsorption is accompanied by overlapping and interaction of electron densities of the adsorbed molecules and the sensing material resulting in the formation of a charge-transfer complex and changes in the conductivity of the latter [1]. In the case of sensing materials based on doped intrinsically conducting polymers (ICPs), this interaction involves conjugated π-electron system of these polymers and, inevitably, affects the quantity and mobility of charge carriers (polarons and bipolarons) in the positively charged polymer backbone [1, 2]. However, a significant influence on the properties of the ICPs (charges, conductivity, morphology, lattice distortions, distance between the macromolecular chains, solubility, *etc*.) is made by the nature and size of dopant anions [3, 4], which can also act as specific binding sites in the interaction of the doped intrinsically conducting polymer with analyte molecules [5]. The ICPs properties are strongly influenced and often improved in nano-composites of them with different nanomaterials (carbon nanotubes, graphene oxide, graphene, nanoparticles of metal oxides and chalcogenides, metal or polymer particles, *etc*.) especially with a core-shell morphology [6, 7]. The degree of this effect depends on the strength and nature of intermolecular interactions of the ICP component (shell) with the surface of the core (nanomaterial particle) and the conditions of synthesis of these materials [6]. It was shown, in particular, that the oxidation degree and the number of charge carriers (polarons and bipolarons) in a doped polyaniline (PANI) [8] and poly (3-methylthiophene) (P3MT) [9]

components of nanocomposites of them with titania and polyvinylidene fluoride (PVDF), respectively, substantially differed from those of the pure doped PANI and P3MT, thus indicating the differences in their conductivity and sensory properties. In the case of nanocomposites of ICPs with inorganic semiconductors or metals, the ICPs sensing properties are strongly enhanced due to formation of *p-n* or Schottky heterojunctions, respectively [10, 11]. These effects depend not only on ICP but on the nature of the core material as well. In particular, significant differences in the conductivity, morphology, ordering of the P3MT-Cl phase in the shells of P3MT-Cl core-shell nanocomposites with PVDF and multi-walled carbon nanotubes (MWCNTs) and their sensitivity to the simulants of some nerve agents and mustard gas were recently found [12]. Moreover, it was shown that the sensor responses of the MWCNTs/P3MT-Cl nanocomposites are controlled by a partial charge transfer if the difference between their work function and the electronegativity of the analyte molecules does not exceed 0.3 eV. This important finding [12] allows us to suggest that these responses can be additionally affected by directed tuning or modifying the work function and conductivity of the nanocomposites of sensory conducting polymers by changing their surface states and, probably, by tuning interactions between the ICP shell and the core of the nanocomposite. These changes can be made by different methods having their own advantages and disadvantages. In particular, these methods can be realized on a stage of ICP synthesis as it was shown *e.g.* for electrochemical or chemical polymerization of 3,4-ethylenedioxythiophene (EDOT) in the presence of different ionic liquids [13], or of pyrrole in a solution of cyclodextrin sodium salts [14] or calixarenes [15], or in a solution containing both salicylate and molybdate anions [16], *etc.* However, the method, which is based on use of such additives, needs specific procedures and preparations and, inevitably, results in the presence (and/or even in chemical grafting in specific cases) of the modifying additive in the whole bulk of this polymer thus affecting all its properties. At the same time, the gas sensing application works mainly with surface states of the sensitive material.

Naturally, tuning of surface states of sensory ICPs based materials can be realized by using various co-solvents in the film formation process as it was demonstrated for solutions of PEDOT:PSS and its composites (*e.g.* [17–19]). Alternatively, the surface states can be tuned by post-treating the ICP based films with various solvents (ionic liquid and methanol) [20, 21] or reagents (hyaluronic acid and crown ethers) [22, 23]. In particular, addition of up to 5 wt.% of dimethyl sulfoxide (DMSO) in a PEDOT:PSS and poly(ethylene oxide) (PEO) joint solution resulted in a decrease of the sheet resistivity of the PEDOT:PSS/PEO composite films from ~172300 to ~706 Ohm/sq. The sheet resistivity increased to ~ 1954 Ohm/sq at 10 wt.% DMSO concentration [18]. These changes of conductivity were accompanied by similar changes in the work function of the composite films [18]. Simple post-treatment of a spin-coated film of a blend of PEDOT:PSS with polyacrylic acid (at their 20/80 wt. ratio) by methanol resulted in an increase of the film conductivity from 13 to 125 $S \cdot cm^{-1}$ and enhancement of its pressure sensitivity [21]. Modification of the surface of doped sensory ICPs by crown esters [23] was realized in a similar way by submerging polypyrrole (PPy) coated polyester fibers (PPy-C) in methanol solutions of different crown esters for 5 min followed by drying in atmospheric conditions. This treatment increased the resistivity of the PPy-C composite fibers as well as significantly enhanced the sensitivity and selectivity of PPy-C to some amines probably due to the presence of high quantity of oxygen atoms in the cycles and benzo- or dicyclohexyl-substituents [23].

The above-discussed results on tuning electrical and sensing properties of ICPs and their nanocomposites by treatments with solvents or reagents suggest that this approach may be enhanced through modification of these materials by reagents with own high functionality and ability to sense or attract and fix various gases. Among such reagents, various calixarenes (CA), being organic macrocycles with phenol units unified in the cycle with methylene links and having internal hydrophobic cavities [24], are important. The calixarenes have different shapes and sizes predetermined by the quantity of phenol units and nature of substituents. Due to their specific recognition and adsorption properties, calixarenes may be used in a variety of applications, in particular, in gas sensors [25, 26]. A highly effective way to realize gas sensing capability of calixarenes is application of them in a form of thin layers in the quartz crystal microbalance method, which can register *in situ* changes in the weight of these layers when they adsorb or desorb gas analytes [27]. To the best of our knowledge, a promising gas sensing application of calixarenes for modification of ICPs or their composites was shown only in a few papers [28–30]. In particular, Langmuir–Blodgett (LB) films of mixtures of PANI (emeraldine base) and phosphorylated calix[4]resorcinolarene derivative were prepared through their joint solutions [280]. The as-deposited LB films were insulating and became conducting after doping with HCl. Interestingly, the films with less than 20% of calixarene interacted with HCl like pure dedoped PANI. What is more interesting, and was mentioned only in [28], such LB film composites with 20% of CA were much more sensitive to slightly volatile hydrophobic phenylethylamine and far less sensitive to moisture than the mentioned PANI. This allows us to conclude that the molecular recognition capability of the used calixarene made own input in a general sensor response of the LB films prepared in [28]. Another interesting approach consisted in grafting of specific calixarene moieties to an ICP monomer, in particular, to thiophene derivatives, followed by their chemical polymerization in the presence of single-walled carbon nanotubes [29] or by electrochemical polymerization [30] with formation of the modified substituted polythiophenes with capability to discriminate xylene isomers or methane, respectively.

To the best knowledge of us, this work is a first attempt to modify and enhance sensory properties of a chemoresistive conductive binary core-shell nanocomposite of MWCNTs and doped PPy by treating in joint dispersions. Such treatment leads to a physico-chemical interaction with functionalized calixarenes, namely calix[4]arene methylene-bis-phosphonic acid octasodium salt (CPA) and calix[4]arene sulfonic acid (CSA). To disclose how such treatment can work, we show here-in-after the preliminary characterization of the formed ternary nanocomposites (MWCNT/PPy/calix[4]arenes) by transmission electron microscopy (TEM), Fourier transform infrared (FTIR) spectroscopy, and measurements of conductivity and sensor characteristics.

The calix[4]arenes considered in this work differ by functional groups in *p*-positions of their phenolic units. In particular, 8 phosphonic acid groups (an octasodium salt) are in CPA and 4 sulfonic acid groups are in CSA (Fig. 1). These groups should dissociate in solutions and provide free anions. This means that, in our case, adsorption of these calixarenes is also facilitated by Coulomb attraction of their anions to the positively charged doped PPy in the shells covering the carbon nanotubes.

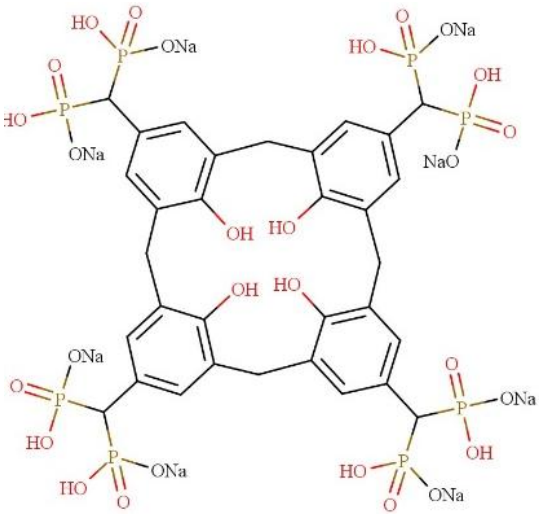

Calix[4]arene methylene-bis-phosphonic acid octasodium salt (CPA)

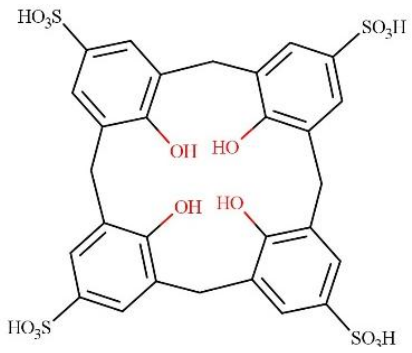

Calix[4]arene sulfonic acid (CSA)

Fig. 1. Molecular structures of the calixarenes.

We also expect that aromaticity and functional groups of these calix[4]arenes can not only facilitate adsorption of them on the surface of nanocomposite particles by intermolecular interactions (π–π stacking, hydrogen bonding) but also change a distribution of the electron density in the nanocomposite components and, therefore, improve the sensitivity of the MWCNT/PPy nanocomposite.

2. Experimental

2.1. Materials and synthesis of nanocomposite MWCNT/PPy

The nanocomposite was synthesized by a similar method to the earlier described one [3] but with some modifications. Namely, chemical oxidative polymerization of pyrrole (Py) was run in an aqueous dispersion of graphitized MWCNTs (Arkema). Before this, a solution of 1.27 g of the oxidant iron(III) p-toluenesulfonate $Fe(TS)_3$ (Sigma-Aldrich) in 26.2 ml of distilled water was prepared and pre-cooled in a thermostat Huber to 1-2 °C. A dispersion of 0.1 g of MWCNTs with 0.054 g of Py (Merck) in 10 ml of distilled water was prepared and pre-cooled to 1-2° for 1.5 h under vigorous stirring. Then this dispersion was slowly added to the oxidant solution and the joint polymerization mixture was stirred with a magnetic stirrer under 250 rpm at 1-2 °C for 5 h. After this, the mixture was filtrated to separate the synthesized MWCNT/PPy-TS nanocomposite. The nanocomposite was washed with a surplus of water first and then by 15 ml of ethanol on a filter. The separated nanocomposite slurry was dried in air for 1 day and under dynamic vacuum at 60 °C for 3 h thereafter.

CPA and CSA were synthesized in the Institute of Organic Chemistry of the NAS of Ukraine by the methods described in [31] and [32], respectively.

2.2. Fabrication of sensor elements

First, joint dispersions of the sensitive MWCNT/PPy-TS nanocomposite and calix[4]arenes in an ethanol-water mixture were prepared by ultrasonication for 2.5 h at a temperature not higher than 18 °C. The dispersions contained 0.08 wt./vol.% of the synthesized MWCNT/PPy-TS nanocomposite and 0…0.15 wt.% of the calixarenes that formed joint ternary nanocomposites upon drying.

Then the sensor elements were prepared by dropping 0.2…0.4 μl of these dispersions onto gold raster electrodes formed on glass–ceramic substrates followed by drying for 40 min at 60 °C and keeping for ~ 24 h at room temperature before measurements.

2.3. Methods and sensor measurements

The TEM images of the pristine MWCNTs and their nanocomposite with PPy-TS were obtained using a TEM microscope JEOL JEM-1400. The FTIR spectra of the samples in pellets with KBr were measured using a Bruker Vertex 70 spectrometer. The *dc* conductivities of the MWCNT/PPy-TS nanocomposite and its mixtures with calix[4]arenes were estimated by a standard two-probe

technique on small pellets (the diameter of 2.7 mm and the thicknesses in the range of 270 to 400 μm). This technique was chosen due to the possibility to work with small quantities of the samples.

Gas sensing properties of the nanocomposites were investigated with the help of the developed earlier injection system and experimental setup [12, 27] by monitoring the changes of the sample resistances in vapors of isopropanol (100…10000 ppm) and ammonia (5…50 ppm). The responses were defined as relative variations of the resistance R of the sensor exposed to an analyte compared with the initial resistance value R_0, $(R - R_0/R_0) \times 100\%$, at ambient temperature and relative humidity of ca. 50%. The responses were recorded during 2 min. We defined the sensor response time as the time needed to reach a plateau of the sensor response (T100%). The recovery time of the sensor was defined as the time needed to reach 25% of the sensor response.

3. Results and discussion

3.1. Characterization of the nanocomposites

3.1.1. Morphology

The TEM images of the pristine MWCNTs and their nanocomposite with PPy-TS reveal the difference in their surface morphology and thicknesses (Fig. 2). The former show a smooth, clean surface and have thicknesses in the range of around 12…20 nm (Fig. 2a). The latter are characterized by an uneven surface coated with small irregularities and have the increased thicknesses in the range of around 20…30 nm. The higher thickness in the latter case is obviously due to the presence of the PPy-TS shells (Fig. 2b). Moreover, in the case of the nanocomposite, a few separate polymeric agglomerated nanoparticles, apparently, of PPy-TS are observed (Fig. 2b).

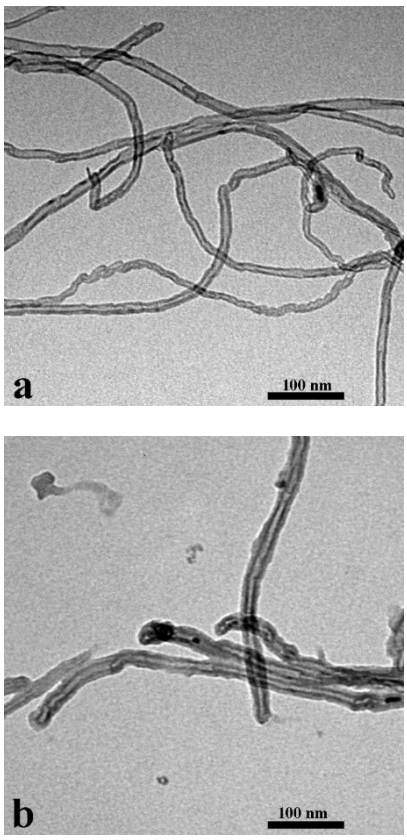

Fig. 2. TEM images of the parent MWCNTs (a) and their core-shell nanocomposite MWCNT/PPy-TS (b).

It should be emphasized here that the TEM visualization (Fig. 2b) shows that the mentioned shells are practically continuous and, therefore, insulate the MWCNTs surface from direct contact and interactions with surrounding media (liquid or gaseous). The averaged thicknesses of the shells lie in the range of around 3 to 6 nm. This means during the preparation of joint dispersions of the MWCNT/PPy-TS nanocomposite and the calixarenes, large functionalized aromatic anions of the latter will adsorb only on the surface of the continuous PPy-TS shells and, therefore, modify electrophysical state (charge carriers, conductivity, work function, *etc*.) of the positively charged PPy units by Coulomb and intermolecular interactions. As a consequence, we may expect that the sensing behavior of the MWCNT/PPy-TS modified by the calixarenes will be changed, too.

3.1.2. Molecular structure of the nanocomposites. FTIR spectra

The suggested above physico-chemical interactions of the charged doped PPy with the functionalized calixarenes adsorbed on the PPy-TS shells of the MWCNT/PPy-TS core-shell nanocomposite are clearly revealed by the changes in the characteristic bands in their FTIR spectra (Fig. 3). In particular, characteristic bands of the doped PPy in the spectrum of the MWCNT/PPy-TS nanocomposite at around 1531, 1450, 1300, 963 cm^{-1} are assigned to the C–C/C=C and C–N/C=C stretching vibrations in the ring, the C–H and C–N in-plane bending in the region of 1400 to 1250 cm^{-1}, and to the C–C out-of-plane ring-deformation vibration, respectively [33–35]. There are also two bands at about 1165 and 1035 cm^{-1} in the region of 1250 to 1000 cm^{-1}. The former corresponds to one of the most intense breathing vibrations of a pyrrole ring. For the doped PPy spectrum, it overlaps with the absorption bands of polarons (~1218 cm^{-1}), bipolarons (~1165 cm^{-1}) and the SO_3 asymmetric stretching vibration band of a tosylate anion (~1183 cm^{-1}). The narrow band at 1035 cm^{-1} is assigned to the combination of CCH, CNH bendings and SO_3 symmetric stretching vibrations. The weak bands with the maxima at 2919 and 2848 cm^{-1} are assigned to C–H asymmetric and symmetric stretching vibrations, respectively, of a CH_3 group in a tosylate anion.

The characteristic intense bands of the calixarenes CPA/CSA at 3261/3189 cm^{-1} and 1600/1600 cm^{-1}, and the doublet at 1482 cm^{-1} and 1462/1471 cm^{-1} with the shoulder at 1460, 902/895 cm^{-1} correspond to stretching vibrations of intra-molecular hydrogen-bonded O–H group at the upper rim of the calixarene, stretching vibrations of aromatic ring C–C and asymmetric deformation vibrations of methylene groups, respectively [36–38].

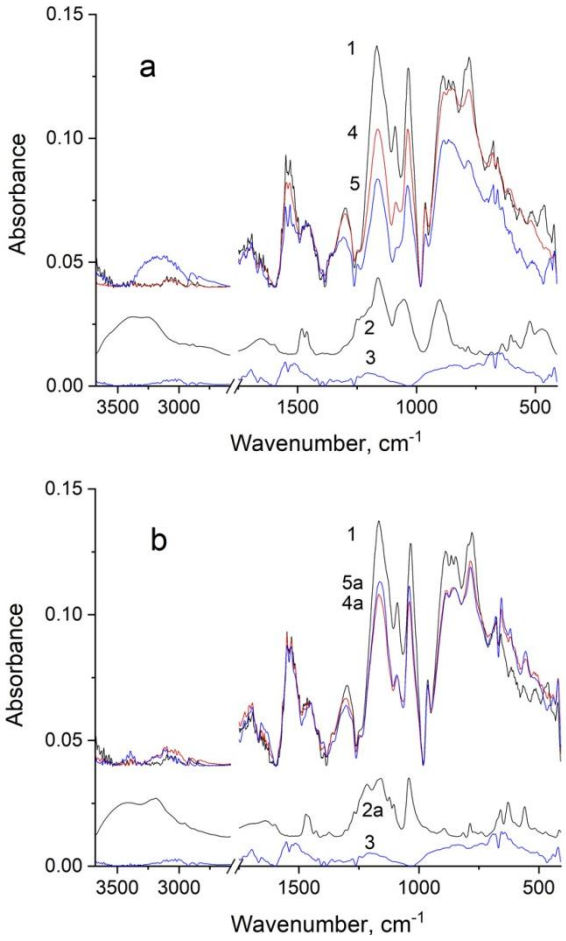

Fig. 3. FTIR spectra of MWCNT/PPy-TS NC (*1*), CPA (*2*), CSA (*2a*), MWCNTs (*3*), MWCNT/PPy-TS/CPA1 NC (*4*), MWCNT/PPy-TS/CPA2 NC (*5*), MWCNT/PPy-TS/CSA1 NC (*4a*), and MWCNT/PPy-TS/CSA2 NC (*5a*). The spectra *1*, *4*, *5*, *4a* and *5a* were normalized to the same absorbance of C–N stretching vibrations at ca. 1450 cm^{-1}.

Asymmetric and symmetric stretching vibrations of CH_2 corresponding to the peaks at 2954 and 2884/2880 cm^{-1} provide low-intensity bands. The O–H stretching vibrations of phosphonic acid groups of the CPA manifest themselves as a shoulder near 2710 cm^{-1}. The bands at 3380/3416 and 1655/1644 cm^{-1} in the FTIR spectra are due to stretching and deformation vibrations of water molecules, which can interact not only with phenolic and phosphonate/ sulfonate groups but are also engaged in OH·aromatic-π can interact not only with phenolic and phosphonate/sulfonate groups but are also engaged in OH·aromatic-π hydrogen bonding in the cavity in the absence of a hydrophobic guest [39]. Binding of a water molecule in the cavity of a calix[4]arene is accompanied by coordination of the oxygen atom of this entrapped molecule with two water molecules outside the cavity. The strong bands at 1162/1158 and 1053/1042 cm^{-1} may be related to a superposition of in-plane bending of aromatic CH groups and bending vibrations of CCH groups with asymmetric and symmetric stretching vibrations of PO_3/SO_2 groups of hydrated monosodium phosphonate/sulphonic acid ($R_1PO_3^{2-}Na,H_3O^+/RSO_3\text{-}H_3O^+$), respectively [36, 39, 40].

However, one can see noticeable changes in the intensity of a number of the characteristic bands of the doped PPy in the ternary (joint) nanocomposites MWCNT/PPy-TS/calixarene. These changes strongly depend on the nature of the calixarenes (Fig. 3). In particular, it was shown both experimentally and theoretically that the intensity ratio of the absorption bands of doped PPy at 1531 and 1450 cm^{-1} (I_{1531}/I_{1450}) is inversely proportional to the change in the π-conjugation length along the polymer chains [41, 42]. In our case, the intensity of the band at about 1531 cm^{-1} decreases quite strongly relative to the band at 1450 cm^{-1} in the case of CPA. However, this effect, even though quite noticeable too, is weaker in the CSA case (Table 1). It should be noted here that the calixarene bands at 1482/1471 cm^{-1} can make a small absorption contribution to the PPy band at 1450 cm^{-1}. However, absence of a noticeable increase in the intensity of the 1480 cm^{-1} band in the spectra *4*, *5* and *4a*, *5a* indicates insignificance of this contribution. Therefore, the mentioned contribution cannot cause the observed changes. This fact suggests that the observed decrease in the I_{1531}/I_{1450} ratio (Table 1) is due to an increase in the π-conjugation length of PPy.

According to known theoretical predictions, increase in the π-conjugation length and a parallel increase in the oxidation degree should cause broadening and shift of the bands associated with vibrations of pyrrole rings [42]. It was experimentally confirmed that the bands at 1531 and 1167 cm^{-1} shifted to lower wavenumbers with increasing PPy oxidation degree [43]. Moreover, the intensity of the bands in the region of 1600 to 900 cm^{-1} grew with increasing the oxidation degree [44].

Table 1. Intensity ratio and position of some characteristic bands of PPy.

Sample	I_{1531}/I_{1450}	I_{1450}/I_{1165}	$\nu_{C-C/C=C}$, cm^{-1}	Ring breathing, cm^{-1}
MWCNT/PPy-TS	2.05	3.89	1531	1167
MWCNT/PPy-TS/CPA1	1.68	2.55	1533	1163
MWCNT/PPy-TS/CPA2	1.33	1.74	1532	1166
MWCNT/PPy-TS/CSA1	2.01	2.75	1531	1167
MWCNT/PPy-TS/CSA2	1.89	2.92	1532	1162

The normalized intensity of the doped PPy related bands in the spectra of the MWCNT/PPy-TS/CPA and MWCNT/PPy-TS/CSA ternary nanocomposites in the region of 1400 to 1000 cm^{-1} noticeably decreased (Fig. 3). This drop in the intensity may correspond to a decrease of the dipole moments of the PPy units due to charge redistribution in the course of intermolecular interactions with large adsorbed calixarene ions and/or due to partial replacement of the TS doping anions by them. This assumption is supported by the fact that the drop is significantly stronger in the case of CPA with more polar functional groups than in the case of CSA as can be clearly seen from the intensity ratio of the absorption bands (I_{1450}/I_{1165}) (Table 1). It is important that the interactions only slightly changed the positions (1…5 cm^{-1}) of these bands in the spectra. This phenomenon suggests that adsorption and specific interactions of the calixarenes with the doped PPy shell affected mainly charge distribution along the PPy chains but not bond strengths (force constants) in the charged PPy rings. Consequently, one may suggest an insignificant decrease in the doping degree of the PPy, which can be stronger in the case of the CPA due to the increased pH of the aqueous medium, from which the CPA is adsorbed. The pH value is approximately equal to 4 taking into account the first p*K*a of the phosphonic acid function ranging from 1.1 to 2.3 and the second acidity with a p*K*a ranging from 5.3 to 7.2 [44]. The increased pH value can also cause some deprotonation of the PPy and a slight decrease of the conductivity [45].

The changes in the spectroscopic characteristics of calixarenes after their adsorption on the MWCNT/PPy-TS composite can also be observed in the region above 2500 cm^{-1}, where there are no strong MWCNT/PPy-TS bands. In particular, the H_2O stretching vibration band at 3380 cm^{-1} in the spectra of MWCNT/PPy-TS/CPA and MWCNT/PPy-TS/CSA disappears in most cases, thus indicating a preference for coordination of phenolic and phosphonate/sulphonate groups with the structural fragments of the MWCNT/PPy-TS composite.

Analysis of the spectral changes in the region of 3000–2500 cm^{-1} shows a decrease in the intensity of the bands at 2919 and 2848 cm^{-1} in the spectra of the composites with calixarenes corresponding to stretching vibrations of CH_3 groups in tosylate anions and, in addition, absence of absorption at 2710 cm^{-1} (ν_{O-H} of P–OH) in the spectrum of the MWCNT/PPy-TS/CPA1 (without CPA excess). Such changes confirm the above discussed partial replacement of the tosylate anions by phosphonate and sulphonate anions of CPA and CSA:

$$\text{CPA}: \quad \text{R}-\text{PO(OH)(ONa)} + \text{PPy - TS} \rightarrow$$
$$\rightarrow \text{PPy}^{+} \text{ - R} - \text{PO}_3^{2-} + \text{TSA} + \text{TSNa}$$
$$\text{CSA}: \quad \text{R}_1 - \text{SO}_3\text{H} + \text{PPy - TS} \rightarrow \text{PPy}^{+} \text{ - R}_1 - \text{SO}_3^{-} + \text{TSA}$$

The possibility of a phosphonate anion R–PO_3^{2-} to take part in doping of PPy is confirmed by the fact that the second p*K*a of the phosphonic acid function is less than 7.2 [44]. Therefore, it should not cause significant dedoping of the PPy, which occurs at the pH values above 9 [45]. Substitution of TS^- by R–PO_3^{2-} can probably be facilitated by donor-acceptor interaction of phosphoryl oxygen with electron-deficient fragments of the PPy (polaron or bipolaron), which are essentially the Lewis acids:

$$\text{P=O} \rightarrow \pi \text{ of } \text{PPy}^{+}.$$

Coordination of the phosphoryl oxygens to Lewis acid sites of the PPy will facilitate complexation of tridentate units. However, strong absorption of the PPy in the region of 1250 to 900 cm^{-1} does not allow us to distinguish the type of phosphonate coupling.

Adsorption of calixarenes on the nanocomposite results in a red shift of their band corresponding to O–H stretching vibrations in the spectra of the MWCNT/ PPy-TS/CPA by 80 cm^{-1} (from 3261 to 3180 cm^{-1}) and in the spectra of the MWCNT/PPy-TS/SCA by 10 cm^{-1} (from 3189 to 3179 cm^{-1}). Such a strong difference confirms the stronger interaction of CPA with the MWCNT/PPy-TS compared to CSA. Moreover, taking into account the fact that one of the phenolic OH groups of calixarenes is very acidic (pK_{a1} = 1…2.9) [46], it may be assumed that a phenolate anion is formed. This ion can participate in the electrostatic and anion-π interactions with the polypyrrole chain. As an indirect confirmation of the formation of phenolate anion of calixarenes, one can consider the absorption band of this anion in the region of about 3180 cm^{-1} [47].

3.2. Electrical and sensing properties of the nanocomposites

As one can see from Table 2, the dried ternary MWCNT/PPy-TS/calix[4]arenes nanocomposites have lowered conductivities as compared with that of the parent binary MWCNT/PPy-TS.

However, while the conductivity drop is enhanced with an increase of both the calix[4]arenes concentrations and contents in the ternary nanocomposites, this drop is much stronger in the case of CPA containing a high amount of phosphoric groups as compared to CSA (Table 1). These drop effects may be explained by dilution of the conducting MWCNT/PPy-TS binary nanocomposite with the low-conducting calix[4]arenes. Indeed, it is known that calixarenes have a very low conductivity and, therefore, can interfere with contacts between the conducting nanotubes of the MWCNT/PPy-TS in their joint nanocomposites. However, taking into account much lower molar concentrations of CPA and, therefore, smaller quantities of its anions in the ternary nanocomposite as compared to those of the CSA case, one may assume that the conductivity drop is caused not only by dilution of the conducting MWCNT/PPy-TS component but also by specific interactions of the calix[4]arenes moieties with the PPy-TS shells on the MWCNTs cores. This assumption agrees with the above discussed FTIR spectra of the nanocomposites and pure components, which suggested an increased π-conjugation degree in the PPy component and decreased dipole moments of the PPy units, probably due to additional interactions with the calixarenes additives, which results in the changes of the properties of the PPy based nanocomposite.

Table 2. Electrical properties of the MWCNT/PPy-TS binary nanocomposite and its ternary nanocomposites with calix[4]arenes.

Sam-ple	Components of the nanocomposites	Concentration ratio of the components in the dispersion, wt.%/v.%	Molar concen-tration of calix[4]arenes, mol/L	Mass ratio of the component contents in the dry nanocomposite	Resisti-vity, Ohm·cm	Conduc-tivity, S/cm
1	MWCNT/PPy-TS	n/a		n/a	2.024	0.494
2	MWCNT/PPy-TS + CSA	0.08:0.05	$6.72 \cdot 10^{-4}$	8:5	2.762	0.362
3	MWCNT/PPy-TS + CSA	0.08:0.15	$20.16 \cdot 10^{-4}$	8:15	5.155	0.194
4	MWCNT/PPy-TS + CPA	0.08:0.05	$3.86 \cdot 10^{-4}$	8:5	4.739	0.211
5	MWCNT/PPy-TS + CPA	0.08:0.15	$11.57 \cdot 10^{-4}$	8:15	6.993	0.143

Indeed, enhancement of the sensing properties of the conducting ternary nanocomposites MWCNT/PPy-TS/CSA and MWCNT/PPy-TS/CPA confirm the existence of intermolecular interactions of the calix[4]arenes with other components. In particular, despite the fact that these nanocomposites have a decreased conductivity compared to the parent binary MWCNT/PPy-TS nanocomposite (Table 1), their responses to VOC (shown here on the example of isopropanol) and VIC (shown here on the example of ammonia) were enhanced in most cases, although with a significant specificity, which depended on the calix[4]arene nature and concentration as well as on the analyte used (Figs 4 and 5).

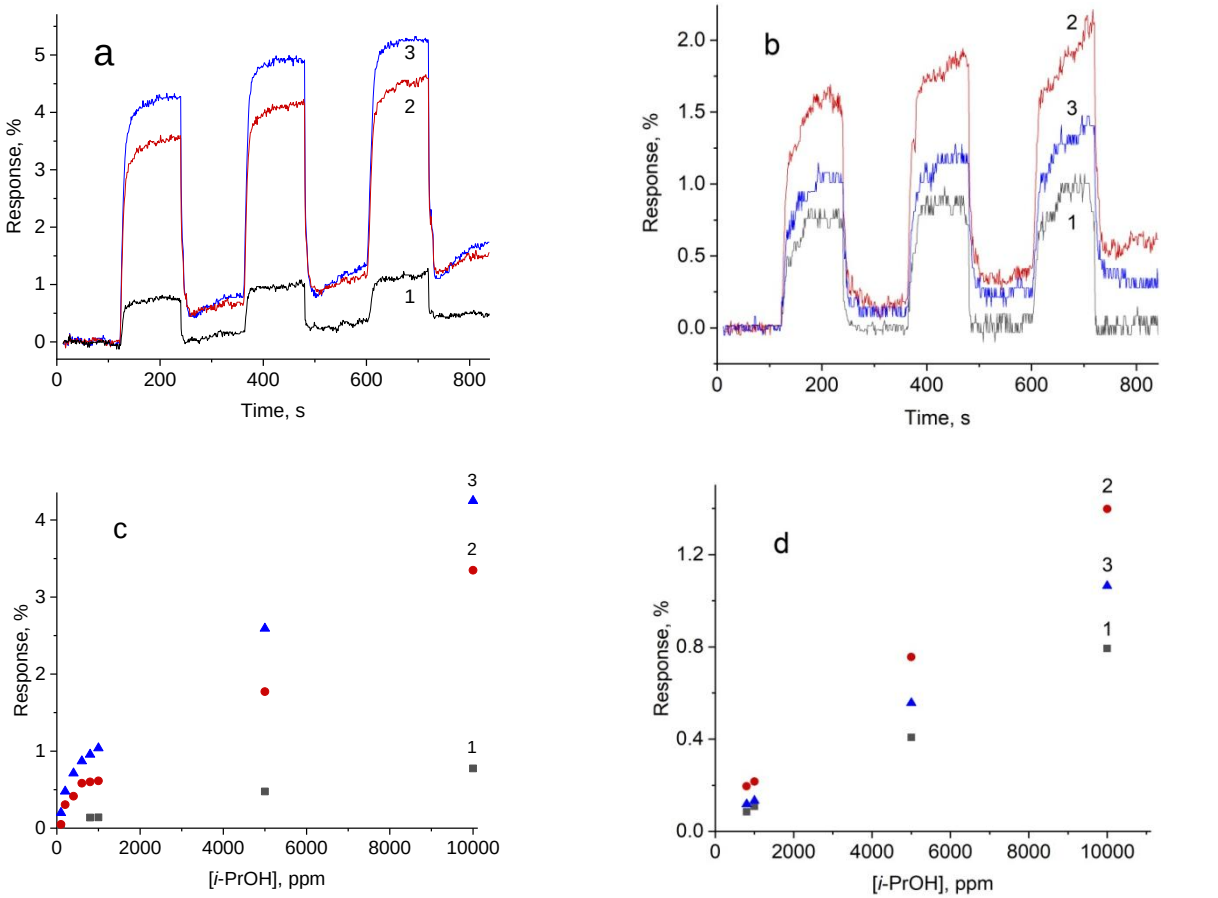

Fig. 4. Effects of the calixarenes additives on the sensitivity of the binary nanocomposite: serial responses of the MWCNT/PPy-TS/CSA (a) and MWCNT/PPy-TS/CPA (b) nanocomposites to 10000 ppm of isopropanol vapors; concentration dependences of the sensor responses of the MWCNT/PPy-TS/CSA (c) and MWCNT/PPy-TS/CPA (d) to isopropanol: *1* – without additives, *2* – 0.05 wt.% of the additives in the 0.08 wt.% of the MWCNT/PPy-TS dispersion, *3* – 0.15 wt.% of the additives in the 0.08 wt.% of the MWCNT/PPy-TS dispersion.

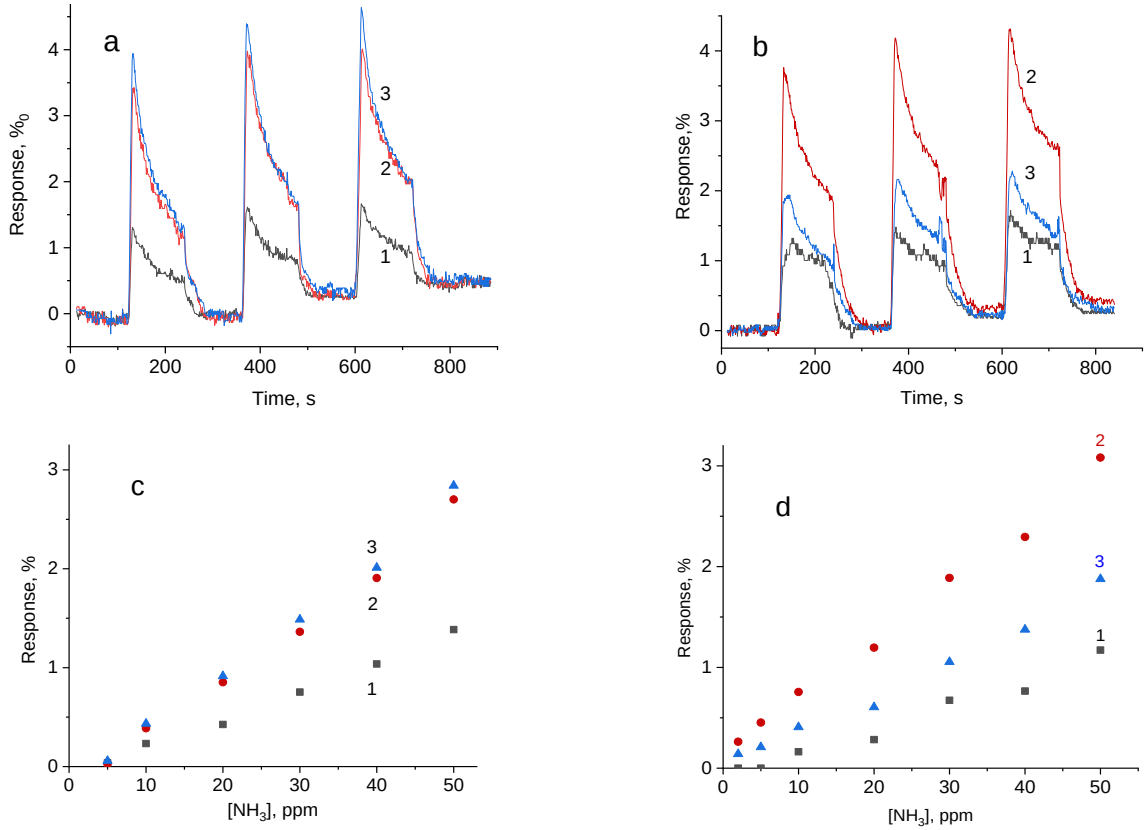

Fig. 5. Effects of the calixarenes additives on the sensitivity of the binary nanocomposite: serial responses of the MWCNT/PPy-TS/CSA (a) and MWCNT/PPy-TS/CPA (b) nanocomposites to 30 ppm of ammonia vapors; concentration dependences of the sensor responses of the MWCNT/PPy-TS/CSA (c) and MWCNT/PPy-TS/CPA (d) to ammonia: *1* – without additives, *2* – 0.05% wt/v. of the additives in the 0.08 wt.% of the MWCNT/PPy-TS dispersion, *3* – 0.15% of the additives in the 0.08% wt/v of the MWCNT/PPy-TS dispersion.

The highest responses to isopropanol were observed for the case of the CSA additives. In particular, these responses to 1000 ppm of isopropanol increased by the factors ~4 and ~7.5 at the CSA concentrations in the dispersions of 0.05% and 0.15% wt/v (Fig. 4a), respectively. In the CPA case, the enhancement of the responses to 1000 ppm of isopropanol was much smaller and, contrary to the CSA case, was even lower (by the factor ~1.2) at the higher concentration (0.15% wt/v) than at the concentration of 0.05% wt/v (by the factor ~2) (Fig. 4b). Such differences in the influence of the calixarenes on the sensing behavior of the nanocomposites emphasize the above described specificity of the calixarenes interaction with the PPy component (see FTIR and conductivity data). These differences also suggest different mechanisms or, at least, significant peculiarities of the adsorption/penetration of isopropanol molecules on/into the doped PPy shells coated by calix[4]arenes layers, which underlies the nanocomposites sensitivity. This suggestion is supported by non-linear and linear concentration dependences of the sensor responses [48, 49] to isopropanol in the cases of CSA and CPA, respectively, as well as by the higher sensitivity in the former case with the detection limit of 100 ppm (under measurements conditions) as compared to 800 ppm in the latter case (Figs 4c, 4d, curves *2* and *3*). In the absence of the calixarenes, the parent binary nanocomposite MWCNT/PPy-TS show a linear concentration dependence with low sensitivity and detection limit of 800 ppm (Figs 4c, 4d, curve *1*).

All the nanocomposites showed a much higher sensitivity to ammonia as compared to that to isopropanol, which is typical for most ICP based sensing materials. They also showed linear concentration dependences in the range of 5 to 50 ppm (Fig. 5). In particular, their responses to 50 ppm of ammonia were in the range of 1 to 3% (Fig. 5), while the responses of the most sensitive MWCNT/PPy-TS/CSA nanocomposite to 50 ppm of isopropanol, estimated from the concentration dependences in Fig. 4, were around 0.1%. Moreover, contrary to the results of the measurements with isopropanol vapor (Fig. 4), the MWCNT/PPy-TS/CSA nanocomposite with 0.05% wt/v of SCA was little less sensitive to ammonia than the MWCNT/PPy-TS/CPA (Figs 5c, 5d). Specifically, the responses of the former nanocomposite to 30 ppm of ammonia increased by the factors ~1.8 and ~2.0 at the SCA concentrations in the dispersions of 0.05% wt/v and 0.15% wt/v, respectively (Fig. 5a). In the case of the CPA, the enhancement of the responses to 30 ppm of ammonia was much smaller and, contrary to the SCA case, was even lower (by the factor ~2.8)

at the higher concentration (0.15% wt/v) than at the concentration of 0.05% wt/v (by the factor ~1.6).

The observed specificity of the sensing behaviors of both ternary nanocomposites MWCNT/PPy-TS/ calix[4]arene unexpectedly disagree with the above discussed FTIR and conductivity data, which revealed much more significant effect of the CPA on the charge destribution, π-conjugation length and doping degree in the doped PPy chains as well as the conductivity of the nanocomposites as compared to that of the CSA. Indeed, based on these data, one could expect much higher sensitivity in the CPA case. At this stage of the research, we cannot confidently explain this unexpected controversy. But we suggest a possible explanation, which takes into account the fact that both calix[4]arenes have the same 3-D macrocycle polyaromatic structure with an internal open free volume (basket) capable of host-gest interactions with different molecules absorbed from a solutions or a gas phase. However, the differences in the nature and quantity of the substituents in the *p*-positions of the phenolic rings of both calix[4]arenes, in agreement with [50], should have a strong effect on both such interactions and the interactions of calix[4]arrene molecules with the charged PPy backbone and dopant anions at a molecular level. They should also influence the space orientation of these molecules and their quantity on the surface of the doped PPy shells.

4. Conclusions

In this work, we found for the first time that addition of functionalized calixarenes to a binary core-shell MWCNT/PPy-TS nanocomposite under conditions of a long ultrasonic treatment of their joint dispersions resulted in the formation of a real joint ternary MWCNT/PPy-TS/CA nanocomposite with strong interactions between the components. The interactions are confirmed by the detailed analysis of the FTIR spectra of the parent binary MWCNT/PPy-TS nanocomposite and its ternary MWCNT/PPy-TS/CA nanocomposite counterparts as well as by conductivity and sensor measurements. The mentioned interactions influenced the conjugation degree of the PPy-TS component of the nanocomposite, changed its doping level, charge carriers quantity and even led to a partial replacement of TS^- dopant anion by anions of the calix[4]arenes. As a consequence, the ternary MWCNT/PPy-TS/CA nanocomposites showed a strong enhancement of the sensitivity of the parent MWCNT/PPy-TS to isopropanol, acetone and ammonia vapors due to the CSA and CPA additives. However, these changes depended on the nature of the functional groups of these CA.

Acknowledgement

This research was supported by the National Research Foundation of Ukraine in the framework of the project 2023.03/0243 “Specific interactions and control of properties of nanocomposites of electrically conductive conjugated polymers for sensor applications” under the Grant Support Agreement No. 180/0243.

References

1. Janata J., Josowicz M. Conducting polymers in electronic chemical sensors. *Nat. Mater*. 2003. **2**. P. 19–24. https://doi.org/10.1038/NMAT768.
2. Haynes A., Gouma P. I. Perspective – conducting polymer hybrids as diagnostic chemosensors. *J. Electrochem. Soc.* 2022. **169**. Art. id. 037513. https://doi.org/10.1149/1945-7111/ac5baf.
3. Ogurtsov N.A., Noskov Yu.V., Kruglyak O.S. *et al*. Effect of the dopant anion and oxidant on the structure and properties of nanocomposites of polypyrrole and carbon nanotubes. *Theor. Experim. Chem*. 2018. **54**. P. 114–121. https://doi.org/10.1007/s11237-018-9554-x.
4. Le T.-H., Kim Y., Yoon H. Electrical and electrochemical properties of conducting polymers. *Polymers.* 2017. **9**. Art. id. 150. https://doi.org/10.3390/polym9040150.
5. Cabala R., Meister V., Potje-Kamloth K. Effect of competitive doping on sensing properties of polypyrrole. *J. Chem. Soc. Faraday Trans.* 1997. **93**. P. 131–137. https://doi.org/10.1039/A604780G.
6. Pud A.A., Ogurtsov N.A., Noskov Yu.V. *et al*. On the importance of interface interactions in core-shell nanocomposites of intrinsically conducting polymers. *SPQEO*. 2019. **22**. P. 470–478. https://doi.org/10.15407/spqeo22.04.470.
7. Zhang W., Cao S., Wu Z. *et al*. High-performance gas sensor of polyaniline/carbon nanotube composites promoted by interface engineering. *Sensors*. 2020. **20**. Art. id. 149. https://doi.org/10.3390/s20010149.
8. Mikhaylov S., Ogurtsov N., Noskov Y. *et al*. Ammonia/amines electronic gas sensors based on hybrid polyaniline-TiO_2 nanocomposites. The effects of titania and the surface active doping acid. *RSC Adv*. 2015. **5**. P. 20218–20226. https://doi.org/10.1039/C4RA16121A.
9. Ogurtsov N.A., Bliznyuk V.N., Mamykin A.V. *et al*. Poly(vinylidene fluoride)/poly (3-methylthiophene) core–shell nanocomposites with improved structural and electronic properties of the conducting polymer component. *Phys. Chem. Chem. Phys.* 2018. **20**. P. 6450–6461. https://doi.org/10.1039/C7CP07604E.
10. Yan Y., Yang G., Xu J.-L. *et al*. Conducting polymer-inorganic nanocomposite-based gas sensors: a review. *Sci. Technol. Adv. Mater*. 2020. **21** P. 768–786. https://doi.org/10.1080/14686996.2020.1820845.
11. Liu X., Zheng W., Kumar R. *et al*. Conducting polymer-based nanostructures for gas sensors. *Coord. Chem. Rev.* 2022. **462**. Art. id. 214517. https://doi.org/10.1016/j.ccr.2022.214517.
12. Ogurtsov N.A., Mamykin A.V., Kukla O.L. *et al*. The impact of interfacial interactions on structural, electronic and sensing properties of poly(3-methylthiophene) in the core-shell nanocomposites. Application to the CWA simulants detection. *Macromol. Mater. Eng.* 2022. **307**. Art. id. 2100762. https://doi.org/10.1002/mame.202100762.

13. Qu K., Dai W., He T. Unique tunability to conducting polymer enabled by ionic liquid doping and its application in nitrite sensing. *J. Electrochem. Soc*. 2022. **169**. Art. id. 106520. https://doi.org/10.6520. 10.1149/1945-7111/ac9b99.
14. Annibaldi V., Hendy G.M., Breslin C.B. Studies on the formation and properties of polypyrrole doped with ionised β-cyclodextrins: influence of the anionic pendants. *J. Solid. State Electrochem.* 2019. **23**. P. 615–626. https://doi.org/10.1007/s10008-018-04171-8.
15. Waghmode B.J., Husain Z., Joshi M. *et al*. Synthesis and study of calixarene-doped polypyrrole-TiO_2/ZnO composites: Antimicrobial activity and electrochemical sensors. *J. Polym. Res.* 2016. **23**. Art. id. 35. https://doi.org/10.1007/s10965-016-0921-9.
16. Trung V.Q., Hung H.M., Khoe L.V. *et al*. Synthesis and characterization of polypyrrole film doped with both molybdate and salicylate and its application in the corrosion protection for low carbon steel. *ACS Omega*. 2022. **7**. P. 19842–19852. https://doi.org/10.1021/acsomega.2c01561.
17. Shahrim N.A., Ahmad Z., Azman A.W. *et al*. Mechanisms for doped PEDOT:PSS electrical conductivity improvement. *Mater. Adv.* 2021. **2**. P. 7118–7138. https://doi.org/10.1039/d1ma00290b.
18. Hwang J., Oh T., Kim S. *et al*. Effect of solvent on electrical conductivity and gas sensitivity of PEDOT: PSS polymer composite films. *J. Appl. Polym. Sci*. 2015. **132**. https://doi.org/10.1002/app.42628.
19. Setiawan R.C., Li D.Y. Tuning the conductivity and electron work function of a spin-coated PEDOT:PSS/PEO nanofilm for enhanced interfacial adhesion. *Langmuir*. 2021. **37**. P. 4924–4932. https://doi.org/10.1021/acs.langmuir.1c00147.
20. Jia Y., Li X., Jiang F. *et al*. Effects of additives and post-treatment on the thermoelectric performance of vapor-phase polymerized PEDOT films. *J. Polym. Sci. Part B*. 2017. **55**. P. 1738–1744. https://doi.org/10.1002/polb.24422.
21. Tseng Y.-T., Lin Y.-C., Shih C.-C. *et al*. Morphology and properties of PEDOT:PSS/soft polymer blends through hydrogen bonding interaction and their pressure sensor application. *J. Mater. Chem. C*. 2020. **8.** P. 6013–6024. https://doi.org/10.1039/d0tc00559b.
22. Cen L., Neoh K.G., Kang E.T. Surface functionalization of electrically conductive polypyrrole film with hyaluronic acid. *Langmuir*. 2008. **18**. P. 8633–8640. https://doi.org/10.1021/la025979b.
23. Alizadeh N., Pirsa S., Mani-Varnosfaderani A., Alizadeh M.S. Design and fabrication of open-tubular array gas sensors based on conducting polypyrrole modified with crown ethers for simultaneous determination of alkylamines. *IEEE Sens. J*. 2015. **15**. P. 4130–4136. https://doi.org/10.1109/JSEN.2015.2411515.
24. Neri P., Sessler J.L., Wang M.-X. (Eds.) *Calixarenes and Beyond*. Springer Cham, 2016. https://doi.org/10.1007/978-3-319-31867-7.
25. Kumar S., Chawla S., Zou M.C. Calixarenes based materials for gas sensing applications: a review. *J. Incl. Phenom. Macrocycl. Chem*. 2017. **88**. P. 129–158. https://doi.org/10.1007/s10847-017-0728-2.
26. Deska M., Dondela B., Sliwa W. Selected applications of calixarene derivatives. *ARKIVOC*. **2015**. P. 393–416. http://doi.org/10.3998/ark.5550190.p008.958.
27. Mamykin A.V., Kukla O.L., Pavluchenko A.S. *et al*. "Electronic nose"-type chemosensory systems for detection of gaseous poisonous substances. *SPQEO*. 2022. **25**. P. 429–440. https://doi.org/10.15407/spqeo25.04.429.
28. Lavrik N.V., De Rossi D., Kazantseva Z.I. *et al*. Composite polyaniline/calixarene Langmuir-Blodgett films for gas sensing. *Nanotechnology*. 1996. **7**. P. 315–319. https://doi.org/10.1088/0957-4484/7/4/002.
29. Wang F., Yang Y., Swager T.M. Molecular recognition for high selectivity in carbon nanotube/polythiophene chemiresistors. *Angew. Chem. Int. Ed.* 2008. **47**. P. 8394–8396. http://doi.org/10.1002/anie.200802762.
30. Lu R.-Q., Luo S.-X.L., He Q. *et al*. Methane detection with a tungsten-calix[4]arene-based conducting polymer embedded sensor array. *Adv. Funct. Mater.* 2020. **31**. Art. id. 2007281. https://doi.org/10.1002/adfm.202007281.
31. Lugovskoy E.V., Gritsenko P.G., Koshel T.A. *et al*. Calix[4]arene methylenebisphosphonic acids as inhibitors of fibrin polymerization. *FEBS J*. 2011. **278**. P. 1244–1251. https://doi.org/10.1111/j.1742-4658.2011.08045.x.
32. Shinkai S., Araki K., Tsubaki T. *et al*. New syntheses of calixarene-p-sulphonates and p-nitrocalixarenes. *J. Chem. Soc. Perkin Trans*. 1987. **1**. P. 2297–2299. https://doi.org/10.1039/P19870002297.
33. Kostić R., Raković D., Stepanyan S.A. *et al*. Vibrational spectroscopy of polypyrrole, theoretical study. *J. Chem. Phys.* 1995. **102**. P. 3104–3109. https://doi.org/10.1063/1.468620.
34. Kofranek M., Kovář T., Karpfen A., Lischka H. *Ab initio* studies on heterocyclic conjugated polymers: Structure and vibrational spectra of pyrrole, oligopyrroles, and polypyrrole. *J. Chem. Phys.* 1992. **96**. P. 4464–4473. https://doi.org/10.1063/1.462809.
35. Christensen P.A., Hamnett A. *In situ* spectroscopic investigations of the growth, electrochemical cycling and overoxidation of polypyrrole in aqueous solution. *Electrochim. Acta*. 1991. **36**. P. 1263–1286. https://doi.org/10.1016/0013-4686(91)80005-S.
36. Larkin P. *Infrared and Raman Spectroscopy: Principles and Spectral Interpretation*. Elsevier, 2017.
37. Amiri A., Babaeie F., Monajjemi M. Vibrational analysis of p-tert-butyl-calix[4]arene conformers by *ab initio* calculations. *Phys. Chem. Liq.* 2008. **46**. P. 379–389. https://doi.org/10.1080/00319100701344610.

38. Furer V.L. Vandyukov A.E., Kleshnina S.R. *et al*. DFT study of conformation, hydrogen bonds, IR, and Raman spectra of the sodium salt of p-hexasulfonatocalix[6]arene. *J. Mol. Struct.* 2021. **1243**. Art. id. 130892. https://doi.org/10.1016/j.molstruc.2021.130892.
39. Atwood J.L., Hamada F., Robinson K.D. *et al*. X-ray diffraction evidence for aromatic π hydrogen bonding to water. *Nature*. 1991. **349**. P. 683–684. https://doi.org/10.1038/349683a0.
40. Gliboff M., Sang L., Knesting K.M. *et al*. Orientation of phenylphosphonic acid self-assembled monolayers on a transparent conductive oxide: a combined NEXAFS, PM-IRRAS, and DFT study. *Langmuir*. 2013. **29**. P. 2166–2174. https://doi.org/10.1021/la304594t.
41. Lei J., Cai Z., Martin C.R. Effect of reagent concentrations used to synthesize polypyrrole on the chemical characteristics and optical and electronic properties of the resulting polymer. *Synth. Met.* 1992. **46**. P. 53–69. https://doi.org/10.1016/0379-6779(92)90318-D.
42. Tian B., Zerbi G. Lattice dynamics and vibrational spectra of pristine and doped polypyrrole: effective conjugation coordinate. *J. Chem. Phys*. 1990. **92**. P. 3892–3898. https://doi.org/10.1063/1.457795.
43. Maia G., Ticianelli E.A., Nart F.C. FTIR investigation of the polypyrrole oxidation in Na_2SO_4 and $NaNO_3$ aqueous solutions. *Z. Phys. Chem*. 1994. **186**. P. 245–257. https://doi.org/10.1524/zpch.1994.186.Part_2.245.
44. Sevrain C.M., Berchel M., Couthon H., Jaffrès P.A. Phosphonic acid: preparation and applications. *Beilstein J. Org. Chem*. 2017. **13**. P. 2186–2213. https://doi.org/10.3762/bjoc.13.219.
45. Pei Q., Qian R. Protonation and deprotonation of polypyrrole chain in aqueous solutions. *Synth. Met.* 1991. **45**. P. 35–48. https://doi.org/10.1016/0379-6779(91)91845-2.
46. Araki K., Iwamoto K., Shinkai S., Matsuda T. "pKa" of calixarenes and analogs in nonaqueous solvents. *Bull. Chem. Soc. Jpn*. 1990. **63**. P. 3480–3485. https://doi.org/10.1246/bcsj.63.3480.
47. Brzezinski B., Urjasz H., Zundel G. Cyclic hydrogen-bonded system with large proton polarizability in calixarenes an FT-IR study. *J. Phys. Chem*. 1996. **100**. P. 9021–9023. https://doi.org/10.1021/jp9535396.
48. Sarkar T. Srinives S., Rodriquez A., Mulchandani A. Single-walled carbon nanotube-calixarene based chemiresistor for volatile organic compounds. *Electroanalysis*. 2018. **30**. P. 2077–2084. http://doi.org/10.1002/elan.201800199.
49. Sarkar T., Srinives S. Single-walled carbon nanotubes-calixarene hybrid for sub-ppm detection of NO_2. *Microelectron. Eng.* 2018. **197**. P. 28–32. https://doi.org/10.1016/j.mee.2018.05.004.
50. Ozmen M., Ozbek Z., Buyukcelebi S. *et al*. Fabrication of Langmuir–Blodgett thin films of calix[4]arenes and their gas sensing properties: Investigation of upper rim *para* substituent effect. *Sens. Act. B: Chem*. 2014. **190**. P. 502–511. https://doi.org/10.1016/j.snb.2013.09.008.

Authors and CV

A.A. Pud, Doctor of Sciences in Polymer Science, Professor, Head of the Department of Chemistry of Functional Materials at the Institute of Bioorganic Chemistry and Petrochemistry. His research interests are in the fields of chemical and electrochemical formation, properties and functioning of intrinsically conducting polymer (ICP) structures in dispersions and solid-phase media, synthesis, properties and applications of multifunctional hybrid (nano)composites of ICP with polymers of other nature and inorganic nanoparticles (semiconductor, dielectric, magnetic).
https://orcid.org/0000-0002-0681-633X

N.A. Ogurtsov, PhD in Chemistry, Senior Researcher at the Institute of Bioorganic Chemistry and Petrochemistry. His current research interests are focused on synthesis of nanocomposites based on conducting polymers and structure–property relationship of these materials.
E-mail: ogurtsov@bpci.kiev.ua,
https://orcid.org/0000-0002-5193-2276

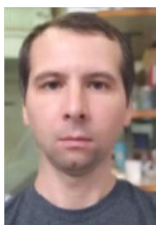

Yu.V. Noskov, PhD in Macromolecular Chemistry, Research Fellow at the Department of Chemistry of Functional Materials of the Institute of Bioorganic Chemistry and Petrochemistry. His scientific interests are focused on synthesis of conjugated polymers and their multifunctional hybrid nanocomposites, nanoparticles and their applications as sensor materials, in solar cells, and drug delivery systems. E-mail: yuriy.noskov@gmail.com, https://orcid.org/0000-0002-4192-1733

O.S. Kruglyak, Engineer at the Department of Chemistry of Functional Materials of the Institute of Bioorganic Chemistry and Petrochemistry. Her current research interests are gas sensory properties of nanocomposites based on various conductive polymers, detection and quantification of specific gases in indoor atmosphere or in ambient. E-mail: o_kruglyak@ukr.net,
https://orcid.org/0000-0003-0704-3436

A.V. Mamykin, Junior Researcher of the Department of Functional Transducers for Sensor Technique at the V. Lashkaryov Institute of Semiconductor Physics. His areas of research are mathematical modeling of electrochemical analytical systems, development of spectral impedance methods for determining physico-chemical parameters of various functional materials, and study of sensory properties of gas-sensitive thin-film layers of electrically conductive composite polymers. E-mail: avmamykin@gmail.com, https://orcid.org/0000-0001-5262-7719

O.L. Kukla, Doctor of Sciences in Physics of Devices, Elements and Systems, Head of the Department of Functional Transducers for Sensor Technique at the V. Lashkaryov Institute of Semiconductor Physics. His areas of research are development and design of chemical gas sensors, biological sensors and sensor arrays for biotechnology, medicine and ecology as well as study of molecular adsorption effects in polymer, biopolymer and composite thin layers. E-mail: alex.le.kukla@gmail.com, https://orcid.org/0000-0003-0261-982X

S.O. Cherenok, Doctor of Chemical Sciences, Head of the Department of Chemistry of Macrocyclic Compounds at the Institute of Organic Chemistry. The area of his research includes supramolecular chemistry of phosphorus-, sulfur- and nitrogen-containing macrocyclic compounds. E-mail: cherenokserhii@gmail.com, https://orcid.org/0000-0003-1736-3062

S.G. Vyshnevskyy, PhD in Organic Chemistry, Researcher at the Macrocyclic Chemistry Department of the Institute of Organic Chemistry. His scientific interests include synthesis of thiocalixarene-based compounds, general organic synthesis and physical chemical investigations. E-mail: vishnev.srg.@gmail.com

V.I. Kalchenko, Doctor of Chemical Sciences, Professor, Academician of the National Academy of Sciences of Ukraine. His scientific interests are chemistry of calixarenes, organophosphorus chemistry, supramolecular chemistry, design and synthesis of novel materials. Nowadays, he holds a position of a Leading Scientist at the Institute of Organic Chemistry. E-mail: vik@ioch.kiev.ua, https://orcid.org/0000-0002-0325-7544

Authors' contributions

Pud A.A.: conceptualization, project administration, resources, writing – original draft, review & editing.
Ogurtsov N.A.: investigation, resources, writing – original draft.
Noskov Yu.V.: investigation, resources.
Kukla O.L.: conceptualization, resources.
Kruglyak O.S.: methodology, data treatment, formal analysis.
Mamykin A.V.: formal analysis, methodology, resources.
Cherenok S.O.: methodology, resources, synthesis.
Vyshnevskyy S.G.: methodology, resources, synthesis.
Kalchenko V.I.: conceptualization, resources, writing – original draft.

Посилення сенсорних властивостей хеморезистивних електропровідних нанокомпозитів вуглецевих нанотрубок і поліпіролу функціоналізованими каліксаренами

О.А. Пуд, Ю.В. Носков, М.О. Огурцов, О.Л. Кукла, О.С. Кругляк, А.В. Мамикін, С.О. Черенок, С.Г.Вишневський, В.І. Кальченко

Анотація. У цій роботі вперше показано модифікацію та покращення сенсорних властивостей хеморезистивного електропровідного нанокомпозиту типу ядро-оболонка з багатошарових вуглецевих нанотрубок (ВНТ) і поліпіролу (ППі), легованого *n*-толуолсульфонатними аніонами (ТС) (ВНТ/ППі-ТС), при тривалій ультразвуковій обробці в спільних дисперсіях і, отже, при фізико-хімічній взаємодії з функціоналізованими каліксаренами (КА), а саме октанатрієвою сіллю калікс[4]арен метилен-біс-фосфонової кислоти (КФА) і калікс[4]аренсульфоновою кислотою (КСА). Взаємодії підтверджено детальним аналізом ФТ-IR спектрів вихідного бінарного нанокомпозиту ВНТ/ППі-ТС та його аналогів потрійних нанокомпозитів ВНТ/ППі-ТС/КА, а також сенсорними вимірюваннями. Останні показали сильне підвищення чутливості ВНТ/ППі-ТС до пари ізопропанолу, ацетону та аміаку за рахунок добавок КСА та КФА, що, однак, залежить від природи функціональних груп цих КА.

Ключові слова: сенсорні нанокомпозити, вуглецеві нанотрубки, поліпірол, калікс[4]арени, взаємодії, підвищення чутливості.